Hydrogen and Helium Atoms and Molecules in an Intense Magnetic Field

Jeremy S. Heyl*, Lars Hernquist†
Lick Observatory, University of California, Santa Cruz, California 95064, USA

We calculate the atomic structure of hydrogen and helium, atoms and molecules in an intense magnetic field, analytically and numerically with a judiciously chosen basis.

31.10.+z, 31.15.-p, 32.60.+i, 97.60.Jd

I. INTRODUCTION

The problem of atoms and molecules in a magnetic field is both a classic example of time-independent perturbation theory and a vexing challenge in the study of neutron stars and white dwarfs. A sufficiently intense magnetic field cannot be treated perturbatively. The spectra and properties of neutron-star atmospheres depend crucially on magnetic field. Indeed, in the intense magnetic field of a neutron star $B \gtrsim 10^{10}$ G the nucleus rather than the field acts as a perturbation. The electron is effectively confined to move along the magnetic field lines.

This work extends classic analytic work on the one-dimensional hydrogen atom [1,2] to form the basis of a perturbative treatment of hydrogen in an intense magnetic field. This analytic treatment yields binding energies for $B \gtrsim 10^{12}$ G whose accuracy rivals that of the recent exhaustive treatment of hydrogen in an magnetic field by Ruder *et al.* [3] with substantially less computational expense.

We also present a straightforward numerical treatment of the hydrogen atom, the hydrogen molecular ion and the helium atom. The electron wavefunction is expanded in a convenient basis, and the Schrödinger equation may be solved approximately by diagonalizing a suitably calculated matrix. The effective potential between the electrons and between the electrons and the nuclei may be determined analytically, expediting the calculation dramatically.

II. THE SINGLE ELECTRON PROBLEM

We begin with the problem of a single electron bound by the combined field of an atomic nucleus and strong external magnetic field. The Hamiltonian for the electron is given by

$$H = \frac{\mathbf{P}^2}{2M} - \frac{Ze^2}{r} - \mu \cdot \mathbf{B} \tag{1}$$

where we have assumed that the nucleus is infinitely massive, M is the mass of the electron and $\mathbf{P} = \mathbf{p} - e/c\,\mathbf{A}$.

To derive the Schrödinger equation for the electron, we make the replacement $\mathbf{p} = -i\hbar\boldsymbol{\nabla}$. We take the magnetic field to point in the z-direction and choose the gauge where $A_\phi = B\rho/2$, $A_\rho = A_z = 0$ and obtain

$$\left(-\frac{\hbar^2}{2M}\boldsymbol{\nabla}^2 - \frac{i\hbar}{2Mc}B|e|\frac{\partial}{\partial\phi} + \frac{1}{8}\frac{e^2}{Mc^2}B^2\rho^2 - \frac{Ze^2}{r} - \frac{\mu}{s}\sigma_z B - E\right)\psi(1) = 0 \tag{2}$$

where 1 denotes the spin and spatial coordinates of the electron *i.e.* $\mathbf{r}_1, \sigma_1$. The spin portion of the wavefunction decouples from the spatial component; therefore, we take the electron spins antialigned with the magnetic field to minimize the total energy, *i.e.* to calculate the ground state.

For $Z = 0$, we recover the equation for a free electron in an external magnetic field which is satisfied by a function of the form

$$\psi_{nmp_z}(\mathbf{r}) = R_{nm}(\rho,\phi)e^{izp_z/\hbar} \tag{3}$$

where

*Current Address: Theoretical Astrophysics, mail code 130-33, California Institute of Technology, Pasadena, CA 91125
†Presidential Faculty Fellow

$$R_{nm}(\rho,\phi) = \frac{1}{a_H^{|m|+1}|m|!}\left[\frac{(|m|+n)!}{2^{|m|+1}\pi n!}\right]^{1/2} \exp\left(-\frac{\rho^2}{4a_H^2}\right)\rho^{|m|}\ {}_1F_1(-n,|m|+1,\rho^2/2a_H^2)e^{im\phi}, \tag{4}$$

where $a_H = \sqrt{\hbar/M\omega_H} = \sqrt{\hbar c/|e|B}$ [4], and ${}_1F_1$ is the confluent hypergeometric function.

It is convenient to define a critical field where the energy of the Landau ground state $\hbar\omega_H/2$ equals the characteristic energy of hydrogen e^2/a_0, where the Bohr radius, $a_0 \approx 0.53\mathring{A}$. The transition to the intense magnetic field regime (IMF) occurs at [5]

$$B_I = 2m^2c\left(\frac{e}{\hbar}\right)^3 \approx 4.701\times 10^9 \text{ G}. \tag{5}$$

We will express field strengths in terms of $\beta = B/B_I$.

For $Z \neq 0$, the complete solution may be expanded in a sum of ψ_{nmp_z} since these form a complete set. However, for sufficiently strong fields, one can treat the Coulomb potential as a perturbation and use the ground Landau state with the appropriate m quantum number as the first approximation to the radial wavefunction; this is known as the adiabatic approximation.

Equivalently, the adiabatic approximation assumes that the Coulomb potential does not effectively mix the Landau states, *i.e.*

$$\left|\frac{\langle R_{nm}|V(r)|R_{n'm}\rangle}{E_n - E'_n}\right| \ll 1. \tag{6}$$

To determine the validity of the adiabatic approximation we calculate this quantity for the first two Landau states and $m = 0$,

$$\left|\frac{\langle R_{00}|V(r)|R_{10}\rangle}{2\alpha^2\beta Mc^2}\right| = \left|\frac{1}{2\alpha^2\beta Mc^2}\frac{1}{2\pi a_H^2}\int_0^\infty -\frac{Ze^2}{\sqrt{z^2+\rho^2}}\left(1-\frac{\rho^2}{2a_H^2}\right)\exp\left(-\frac{\rho^2}{2a_H^2}\right)2\pi\rho\mathrm{d}\rho\right| \tag{7}$$

$$\leq \left|\frac{1}{2\alpha^2\beta Mc^2}\frac{1}{a_H^2}\int_0^\infty -Ze^2\left(1-\frac{\rho^2}{2a_H^2}\right)\exp\left(-\frac{\rho^2}{2a_H^2}\right)\mathrm{d}\rho\right| = \frac{Z}{4}\sqrt{\frac{\pi}{\beta}}. \tag{8}$$

where $\alpha \approx 1/137$ is the fine structure constant. We find for $\beta = 1000$ ($B = 4.7\times 10^{12}$ G), that the Coulomb potential mixes the Landau states of hydrogen by at most 1.4 %. For stronger fields, the mixing is even less important.

In the adiabatic approximation, we assume that

$$\psi_{0m\nu}(1) = R_{0m}(\rho,\phi)Z_{m\nu}(z)\chi(\sigma) \tag{9}$$

where $Z_{m\nu}(z)$ remains to be determined, ν counts the number of nodes in the z wavefunction, and we expect the axial wavefunctions to be different for different values of the magnetic quantum number m. We will use the notation, $|0m\nu\rangle$, to designate the eigenstates.

For $n = 0$, the functions R_{nm} assume a simple form

$$R_{0m}(\rho,\phi) = \frac{1}{\sqrt{2^{|m|+1}\pi|m|!}a_H^{|m|+1}}\rho^{|m|}\exp\left(-\frac{\rho^2}{4a_H^2}\right)e^{im\phi} \tag{10}$$

$$|R_{0m}(\rho,\phi)|^2 = \frac{(-1)^{|m|}}{2\pi|m|!}\frac{1}{a_H^2}\left(\frac{\mathrm{d}}{\mathrm{d}\kappa}\right)^{|m|}\left[\exp\left(-\kappa\frac{\rho^2}{2a_H^2}\right)\right]\Bigg|_{\kappa=1} \tag{11}$$

With these assumptions the functions $Z_{\nu m}(z)$ satisfy a one-dimensional Schrödinger equation,

$$(H_z - E)Z = \left[-\frac{\hbar^2}{2M}\frac{\mathrm{d}^2}{\mathrm{d}z^2} + V_{\mathrm{eff},0m}(z) - E_{\nu m}\right]Z_{\nu m}(z) = 0, \tag{12}$$

where

$$V_{\mathrm{eff},0m}(z) = \langle R|V(r)|R\rangle = \int_0^\infty -\frac{Ze^2}{\sqrt{z^2+\rho^2}}\left|R_{0m}(\rho)\right|^2 2\pi\rho\,\mathrm{d}\rho. \tag{13}$$

Performing the integral yields [6,5]

$$V_{\mathrm{eff},0m}(z) = -\frac{Ze^2}{a_H}\sqrt{\pi/2}\frac{(-1)^{|m|}}{|m|!}\left(\frac{\mathrm{d}}{\mathrm{d}\kappa}\right)^{|m|}\left[\frac{1}{\sqrt{\kappa}}\exp(\kappa z^2/2a_H^2)\mathrm{erfc}(\sqrt{\kappa}|z|/\sqrt{2}a_H)\right]\Bigg|_{\kappa=1} \tag{14}$$

which for large z approaches $-Ze^2/z$. The Schrödinger equation with this potential is not tractable analytically. We can take one of two paths. First, the potential may be replaced by a simpler yet still accurate function. Second, we attempt to solve the Schrödinger equation numerically.

III. ANALYTIC SOLUTION

A. The Approximate Potential

The potential given in Eq. 14 for arbitrary m may be approximated to within 30 % over the entire domain by the much simpler form

$$V_{\mathrm{eff},0m}(z) \approx V_{\mathrm{approx},0m}(z) = -\frac{Ze^2}{|z| + k_m a_H} \tag{15}$$

where

$$k_m = -\frac{Ze^2}{a_H V_{\mathrm{eff},0m}(0)} = \sqrt{2}\frac{\Gamma(|m|+1)}{\Gamma(|m|+\frac{1}{2})} = \sqrt{\frac{2}{\pi}}\frac{2^{|m|}|m|!}{(2|m|-1)!!} \tag{16}$$

The double factorial is defined by $(-1)!! = 1$ and $(2n+1)!! = (2n+1)(2n-1)!!$. For large m, $\frac{1}{2}k_m a_H$ asymptotically approaches $\sqrt{2|m|+1}a_H$, the mean radius of a Landau orbital.

As we see from Fig. 1, the relative difference between the two expressions is largest near $z = k_m a_H$. For $m = 0$, the difference is greater than 5 % from $z = 0.1$ to $z = 10$. We do not expect this approximation to yield eigenvalues accurate to better than $\sim 10\%$ for wavefunctions peaked in this range.

We obtain the following eigenvalue equation with the approximated potential,

$$\left[-\frac{\hbar^2}{2M}\frac{\mathrm{d}^2}{\mathrm{d}z^2} - \frac{Ze^2}{|z| + k_m a_H} - E_{0m\nu}\right] Z(z) = 0. \tag{17}$$

This equation is nearly identical to the Schrödinger equation with a Coulomb potential; therefore, we treat it as a Coulomb problem by using the natural units (Bohr radii for length and Rydbergs for energy),

$$z = \frac{\lambda\!\!\!^{-}_e}{\alpha}\zeta \text{ and } \epsilon = \frac{2E}{\alpha^2 Mc^2} \tag{18}$$

which yields

$$\left[\frac{\mathrm{d}^2}{\mathrm{d}\zeta^2} + \left(\epsilon + \frac{2Z}{|\zeta| + \zeta_m}\right)\right] Z(\zeta) = 0. \tag{19}$$

where $\zeta_m = k_m\sqrt{1/2\beta}$

Again as in the Coulomb problem, we perform the following substitutions

$$n = \frac{1}{\sqrt{-\epsilon}} \text{ and } \xi = \frac{2\zeta}{n}, \tag{20}$$

yielding,

$$\left[\frac{\mathrm{d}^2}{\mathrm{d}\xi^2} + \left(-\frac{1}{4} + \frac{nZ}{|\xi| + \xi_m}\right)\right] Z(\xi) = 0. \tag{21}$$

This equation may be solved in terms of Whittaker's functions [7]. First, we have

$$Z_1(\xi) = A_\pm M_{nZ,1/2}(|\xi| + \xi_m) = A_\pm(|\xi| + \xi_m)\ {}_1F_1(1 - nZ, 2, |\xi| + \xi_m)e^{-(|\xi|+\xi_m)/2} \tag{22}$$

where $A_\pm$ are the normalization constants for $\xi > 0$ and $\xi < 0$ respectively. Unless nZ is an integer, these solutions tend to infinity as ξ goes to infinity.

As with the equation for an unmagnetized Coulomb potential, there exists an additional set of solutions. For the three-dimensional Coulomb problem, this solution diverges at the origin and is unphysical. However, here we can obtain a well behaved solution. By the method of reduction of order, we obtain the alternative solutions,

$$Z_2(\xi) = A_\pm W_{nZ,1/2}(|\xi| + \xi_m) = A_\pm(|\xi| + \xi_m)\ {}_1F_1(1 - nZ, 2, |\xi| + \xi_m)e^{-(|\xi|+\xi_m)/2} \int^{|\xi|+\xi_m} \frac{e^t}{(t\ {}_1F_1(1 - nZ, 2, t))^2} \mathrm{d}t. \tag{23}$$

These solutions agree with earlier treatments of the one-dimensional hydrogen atom [1,2]. For integer values of nZ, the integral in Eq. 23 diverges; therefore, the eigenvalues differ from those of the unmagnetized Coulomb potential. Additionally for the unmagnetized Coulomb potential, $\xi_m = 0$ and the prefactor of $(|\xi| + \xi_m)$ is absent. We find that in this case, this wavefunction diverges as ξ^{-1} near the origin and only the counterparts of the states given by Eq. 22 are physical.

The solutions to Eq. 17 will be made of a linear combination of Z_1 and Z_2. For a given magnetic quantum number m, the excitations along the magnetic field axis will be denoted by ν with $\nu = 0$ being the ground state. Determining the ground eigenvalue of Eq. 21 for a given value of ξ_m proceeds in reverse. Since the ground state is even, we have $A_+ = A_-$ and $Z'(0) = 0$. One first selects a value for $0 < nZ < 1$. To have the correct behavior as $z \to \infty$, we perform the integral of Eq. 23 from $|\xi| + \xi_m$ to ∞ and calculate $Z_{m0}(\xi)$ for $\xi_m = 0$.

With the calculated function, one can determine where $Z'_{m0}(\xi) = 0$ and use this as the value of ξ_m corresponding to the eigenvalue nZ. The value of ξ_m is simply related to the field strength,

$$\beta = \frac{2k_m^2}{\xi_m^2}(-\lambda) \tag{24}$$

B. First-order Binding Energies

As an example we take $Z = 1$ and $n = 1/\sqrt{15.58}$. This corresponds to a bound state ($|000\rangle$) with an energy of 15.58 Ry. We find $\xi_0 = 0.141$ which yields $\beta = 1000$. For $\beta = 1000$, Ruder *et al.* [3] obtain a binding energy for the $m = 0, \nu = 0$ state of 18.60986 Ry. However, it is straightforward to improve upon our estimate of the binding energy by treating the small difference between the approximate and effective potential as a perturbation. We obtain

$$E_{m0}^{(1)} = \langle Z_{m0}|H'|Z_{m0}\rangle \tag{25}$$

where $H' = V_{\text{eff}} - V_{\text{approx}}$. We then obtain the binding energy to first order of 18.48 Ry for $\beta = 1000$.

This technique may also be applied to states with $m < 0$ by using the appropriate value for k_m in Eq. 17. For example, also for $\beta = 1000$ and $m = -1$ ($|0 - 10\rangle$), we obtain the zeroth order binding energy of 10.45 Ry and the first-order corrected value of 13.71 Ry compared to the result of Ruder *et al.* [3] of 13.90394 Ry. Since Eq. 15 is a better approximation to the effective potential for electrons in the $m = 0$ state than in $m > 0$ states we obtain eigenvalues to first order within 0.7 % of the fully numerical treatment for $\beta \geq 1000$ for these states (compared to within 1.4 % for $m = -1$ states).

To calculate the wavefunctions with $\nu > 0$, we calculate $Z_2(\xi)$ for $nZ > 1$ and use the first extremum or zero of $Z_2(\xi)$ as the value of ξ_0 for the even and odd solutions respectively. Fig. 2 depicts $Z_2(\xi)$ for several values of nZ. For nZ between k and $k + 1$, $Z_2(x)$ has k zeros and $k + 1$ extrema. Therefore, we find that the $\nu > 0$ states have zeroth-order binding energies of fractions of a Rydberg. The calculation of $Z_2(\xi)$ is complicated by the fact that the function $Z_1(\xi)$ also has zeros in the range of integration from ξ to ∞ which make Eq. 23 ill defined. To pass over the singularities in the integrand, we integrate the differential equation 21 directly.

For smaller values of nZ in the range k to $k + 1$, the first zeros and extrema approach $\xi = 0$. Therefore, for larger values of β, the zeroth order eigenvalues of the $\nu > 0$ spectrum approach the Bohr energies. The energies of the odd states approach the Bohr energies from below (*i.e.* they are more weakly bound), and the even states with the same number of nodes are yet more weakly bound [2].

Our first-order adiabatic approximation is less accurate for smaller field strengths. For $\beta = 100$ and $m = 0$ ($|000\rangle$), we obtain a first-order corrected eigenvalue of 9.348 Ry compared to the numerically derived value of 9.4531 Ry (a difference of 1.1 %). However, for fields of $B > 5 \times 10^{11}$ G, the wavefunctions and binding energies derived in this section for $m < 3$ and arbitrary ν are sufficiently accurate for all but the most precise analyses.

C. Perturbed Wavefunctions

To obtain first order corrections to the wavefunctions $Z_{m\nu}$ and second order corrections to the binding energies, we follow the standard techniques for time-independent perturbation theory [8]. We must calculate the following quantities

$$H'_{\nu\mu} = \langle Z_{m\nu}|H'|Z_{m\mu}\rangle \tag{26}$$

for a particular value of β. Since both V_{eff} and V_{approx} are symmetric about $z = 0$, $H'_{\nu\mu}$ is zero for ν odd and μ even.

We obtain

$$Z^{(1)}_{m\nu} = \sum_{\mu\neq\nu} \frac{H'_{\mu\nu}}{E^{(0)}_{\nu} - E^{(0)}_{\mu}} Z^{(0)}_{m\mu} \tag{27}$$

and

$$E^{(2)}_{m\nu} = \sum_{\mu\neq\nu} \frac{|H'_{\mu\nu}|^2}{E^{(0)}_{\nu} - E^{(0)}_{\mu}} \tag{28}$$

For $\beta = 1000$, the mixing among the ν states is on the order of a few percent. The second order corrections to the binding energies for the ground ($\nu = 0$) state is 10^{-3} times the first order correction. For the excited states with $\nu < 6$ the second order correction is less than six percent of the first-order correction; we quote the binding energies to first order for the several of the most bound levels of hydrogen for $\beta \geq 1000$ in Table I and depict the wavefunctions to zeroth order for $\beta = 1000$ in Fig. 3.

IV. NUMERICAL SOLUTION

A. The Basis Set

We can make substantial progress by carefully selecting a basis to expand the solutions $Z_{\nu m}$. Specifically, we choose

$$Z_{\mu m}(z) = \sum_{k=0}^{\infty} A_{\mu mk} \mathcal{G}_k(z) \tag{29}$$

where

$$\mathcal{G}_k(z) = \frac{1}{(2\pi)^{1/4}\sqrt{a_Z 2^k k!}} H_k\left(\frac{z}{\sqrt{2}a_Z}\right) \exp\left(-\frac{z^2}{4a_Z^2}\right). \tag{30}$$

$H_k(z)$ are the Hermite polynomials which are orthogonal on the interval $-\infty$ to ∞ with the weighting function $\exp(-z^2)$. The $\mathcal{G}_k$ are the solutions to the Schrödinger equation for a harmonic oscillator potential; consequently, they provide a complete set for expanding the functions $Z_{\nu m}(z)$.

To obtain the coefficients in the expansion, we calculate the matrix

$$M_{kl} = \langle \mathcal{G}_k|H_z|\mathcal{G}_l\rangle \tag{31}$$

which is a function of a_Z and the azimuthal state given by m. We calculate this matrix for $k, l < N$ ($N = 5 - 50$) and diagonalize it. The eigenvalues of this matrix (λ_ν) are $E_{\nu m}$, and the eigenvectors are the coefficients $A_{\nu mk}$ in Eq. 29. Additionally, the functions $Z_{\nu m}(z)$ and $\mathcal{G}_k(z)$ have definite parity; consequently, for even parity solutions to Eq. 12, only the elements of M_{kl} with k and l even need to be calculated. This reduces the size of the matrix from N^2 to $N^2/4$.

Because the number of basis functions used is not infinite, we cannot expect the expansion to span the Hilbert space of solutions to Eq. 12. To estimate the solution, we vary a_Z to minimize the eigenvalue λ_ν corresponding to the bound state that we are interested in. By using an expansion of the form Eq. 29, the binding energies and wavefunctions may be estimated for excited states along the z-axis.

Although the functions $\mathcal{G}_k$ satisfy a much different equation from Eq. 12, if sufficiently many Gauss-Hermite functions are included, we can obtain highly accurate eigenvalues and eigenvectors. For the ground state ($|000\rangle$)

with the first 31 $\mathcal{G}_k$, we obtain a binding energy of 18.5579 Ry at $\beta = 1000$, within a factor of 3×10^{-3} of the result of Ruder *et al.* , 18.60986 Ry. The results are equally accurate for the first excited state ($|001\rangle$); however, states with more nodes require additional terms in the expansion to achieve the same accuracy. Fig. 4 compares the zeroth-order analytic wavefunction with the numerical wavefunction determined by this technique.

Obtaining an additional few parts per thousand in accuracy can only justify a portion of the additional computation required for this numerical technique; however, this technique may be applied to solve the Schrödinger equation for potentials more complicated than Eq. 14.

B. The H_2^+ molecule

Before proceeding to the multi-electron problem, we study the binding energy of the H_2^+ molecule in an intense magnetic field. We restrict our attention to the case where the axis of the molecule is aligned with the magnetic field direction. This system retains the symmetry under parity of hydrogen, so the numerical technique may be applied directly with only two alterations.

The effective potential is now given by

$$V_{\mathrm{eff},0m,\mathrm{H}_2^+}(z) = V_{\mathrm{eff},0m}(z+a) + V_{\mathrm{eff},0m}(z-a) \tag{32}$$

and we must vary the internuclear separation $2a$ to find the minimum binding energy for the entire system (the Born-Oppenheimer approximation, *e.g.* [8]). We find the ground state, $|000\rangle$, at $\beta = 1000$ has a binding energy of 28.3457 Ry, compared to the LeGuillot & Zinn-Justin [9] result of 28.362 Ry. The internuclear separation is $0.1818a_0$; LeGuillot & Zinn-Justin [9] find $0.181a_0$. Fig. 5 depicts the wavefunctions of the ground and first excited state $|0-10\rangle$ for H_2^+.

The accuracy of our analysis is insufficient to determine if the ungerade state is slightly bound or unbound relative to a hydrogen atom plus a proton. However, in the magnetic case, the electron may be excited into the $|0m0\rangle$ states whose axial wavefunctions are similar to that of the $|000\rangle$ state. The $|0-10\rangle$ state is much less bound at 20.4252 Ry than the $|000\rangle$ state (compared to 18.5579 Ry for the H+p system). For stronger fields, the $|0-20\rangle$ and more excited states are bound relative to the H+p system.

Table II depicts the numerical results for the ground and first excited state of H_2^+ in an intense magnetic field. The ratio of the binding energies of the $|000\rangle$ and $|0-10\rangle$ for H_2^+ is approximately equal to the ratio the energies of the same states of hydrogen and the same magnetic field strength. This observation provides a quick way to estimate the energies of the excited states of H_2^+ from the binding energy of the ground state.

Table III presents results calculated for different values of magnetic field. Our values differ by less than 0.5 % for $B \geq 10^{12}$ G and by $\sim 1\%$ for the two weaker fields considered. We see that the first excited state of H_2^+ becomes bound relative to hydrogen atom and a proton at $B \approx 10^{12}$ G. Furthermore, a comparison of Table III with Table 3 of Lopez *et al.* [10] shows that the ungerade state is unbound for $B \geq 10^{11}$ G.

V. THE MULTIPLE ELECTRON PROBLEM

A. Approach and Results

To calculate the atomic structure of multi-electron atoms, we employ a single-configuration Hartree-Fock technique. Specifically, we assume that the multi-electron wavefunction is given by a single Slater determinant of one-electron wavefunctions. These wavefunctions are varied to minimize the total energy of the system given the constraint that each one-electron wavefunction remains normalized.

This minimization results in the following eigenvalue equations for the individual wavefunctions,

$$F(1)\psi_i(1) = \epsilon_i \psi_i(1) \tag{33}$$

where 1 denotes the spin and spatial coordinates of the electron *i.e.* $\mathbf{r}_1, \sigma_1$.

The operator $F(1)$ is the sum of a kinetic and potential energy term

$$F(1) = H_0(1) + V(1) \tag{34}$$

where the kinetic term is given by the one-particle Schrödinger equation of an electron in the Coulomb field of the nucleus.

The potential energy consists of a direct and exchange interaction with the other electrons

$$V(1) = \sum_j \left[J_j(1) - K_j(1) \right] \tag{35}$$

where

$$J_j(1)\psi_i(1) = \left[\int d\tau_2 \psi_j^*(2) \left(\frac{e^2}{r_{12}} \right) \psi_j(2) \right] \psi_i(1) \tag{36}$$

$$K_j(1)\psi_i(1) = \left[\int d\tau_2 \psi_j^*(2) \left(\frac{e^2}{r_{12}} \right) \psi_i(2) \right] \psi_j(1) \tag{37}$$

Rather than solve the eigenvalue equations directly, we calculate the total energy of the system given a set of wavefunctions and minimize this energy by varying the parameters of the wavefunctions.

In a sufficiently strong magnetic field, these equations for the atomic structure become approximately separable in cylindrical coordinates. With this in mind, we take the trial wavefunctions to be of the form

$$\psi_i(1) = Z(z) R(\rho, \phi) \chi(\sigma). \tag{38}$$

Since we are looking for the ground state of these atoms, we take all the electron spins antialigned with the field and the radial wavefunction to be given by $n = 0$ Landau states with each electron occupying a different m state. We obtain

$$\psi_i(1) = Z_i(z) R_{0m_i}(\rho, \phi) \chi_{-\frac{1}{2}}(\sigma) \tag{39}$$

where

$$R_{0m}(\rho, \phi) = \frac{1}{\sqrt{2\pi |m|!}} \frac{1}{a_H} \exp\left(-\frac{\rho^2}{4a_H^2} \right) \left(\frac{\rho}{\sqrt{2} a_H} \right)^{|m|} e^{im\phi} \tag{40}$$

and $a_H = \sqrt{\hbar c/|e|B}$. We suppress the spin portion of the wavefunction and use the natural length and energy units of the problem $a_H, e^2/a_H$.

The total energy of the system is given by

$$E = \sum_i \langle \psi_i(1) | F(1) | \psi_i(1) \rangle \, . \tag{41}$$

To expedite the calculation we can integrate over the known wavefunctions in the ρ and ϕ coordinates. Specifically, we begin with the integral over ϕ in the potential energy terms

$$\langle \psi_i(1) | J_j(1) | \psi_i(1) \rangle = e^2 \int \rho_1 d\rho_1 dz_1 Z_i^*(z_1) R_{0m_i}^*(\rho_1) Z_i(z_1) R_{0m_i}(\rho_1) \tag{42}$$

$$\times \int \rho_2 d\rho_2 dz_2 Z_j^*(z_2) R_{0m_j}^*(\rho_2) Z_j(z_2) R_{0m_j}(\rho_2) f(\rho_1, \rho_2, z_1 - z_2) \tag{43}$$

$$\langle \psi_i(1) | K_j(1) | \psi_i(1) \rangle = e^2 \int \rho_1 d\rho_1 dz_1 Z_i^*(z_1) R_{0m_i}^*(\rho_1) Z_j(z_1) R_{0m_j}(\rho_1) \tag{44}$$

$$\times \int \rho_2 d\rho_2 dz_2 Z_j^*(z_2) R_{0m_j}^*(\rho_2) Z_i(z_2) R_{0m_i}(\rho_2) g(m_i - m_j, \rho_1, \rho_2, z_1 - z_2) \tag{45}$$

where

$$f(\rho_1, \rho_2, z_1 - z_2) = \int d\phi_1 \int d\phi_2 \frac{1}{\sqrt{\rho_1^2 + \rho_2^2 + (z_1 - z_2)^2 - 2\rho_1 \rho_2 \cos(\phi_1 - \phi_2)}} \tag{46}$$

$$g(m_i - m_j, \rho_1, \rho_2, z_1 - z_2) = \int d\phi_1 \int d\phi_2 \frac{e^{i(m_j - m_i)(\phi_1 - \phi_2)}}{\sqrt{\rho_1^2 + \rho_2^2 + (z_1 - z_2)^2 - 2\rho_1 \rho_2 \cos(\phi_1 - \phi_2)}} \tag{47}$$

The expressions for the functions f and g may be simplified by the substitution $\phi_1 - \phi_2 = 2(\beta + \pi/2)$ and the definition

$$k^2 = \frac{4\rho_1\rho_2}{(\rho_1+\rho_2)^2+(z_1-z_2)^2} \tag{48}$$

resulting in

$$f(\rho_1,\rho_2,z_1-z_2) = \frac{8\pi}{\sqrt{(\rho_1+\rho_2)^2+(z_1-z_2)^2}}\int_0^{\pi/2} d\beta \frac{1}{\sqrt{1-k^2\sin^2\beta}} = \frac{8\pi}{\sqrt{(\rho_1+\rho_2)^2+(z_1-z_2)^2}} F\left(\frac{\pi}{2},k\right) \tag{49}$$

$$g(m_i-m_j,\rho_1,\rho_2,z_1-z_2) = \frac{8\pi}{\sqrt{(\rho_1+\rho_2)^2+(z_1-z_2)^2}}\int_0^{\pi/2} d\beta \frac{e^{2i(m_j-m_i)(\beta+\pi/2)}}{\sqrt{1-k^2\sin^2\beta}} \tag{50}$$

$$= \frac{8\pi}{\sqrt{(\rho_1+\rho_2)^2+(z_1-z_2)^2}}\int_0^{\pi/2} d\beta \frac{\cos(2(m_j-m_i)(\beta+\pi/2))}{\sqrt{1-k^2\sin^2\beta}} \tag{51}$$

where $F\left(\frac{\pi}{2},k\right)$ is the complete Legendre elliptic integral of the first kind. The imaginary portion of the integral for g must be zero since the Hamiltonian is hermitian (i.e. unitarity). This may be seen by expanding the denominator in powers of $\sin^2\beta$ and multiplying this series by $i\sin(2(m_i-m_j)(\beta+\pi/2))$. The integral of this term is zero.

Numerical Recipes [11] provides routines to efficiently calculate $F\left(\frac{\pi}{2},k\right) = \texttt{cel}(\sqrt{1-k^2},1,1,1)$ (unfortunately, this routine is absent from the latest edition). Furthermore, for $|m_i-m_j|=1$, we can use the same routine to calculate g,

$$g(\pm1,\rho_1,\rho_2,z_1-z_2) = \frac{8\pi}{\sqrt{(\rho_1+\rho_2)^2+(z_1-z_2)^2}}\texttt{cel}(\sqrt{1-k^2},1,-1,1). \tag{52}$$

For $|m_i-m_j|>1$, we must perform the integral numerically.

Furthermore, we can gain insight on both the functions f and g by expanding them in the limit of large $\Delta z = |z_i - z_j|$.

$$f(\rho_1,\rho_2,z_1-z_2) = (2\pi)^2\left[\frac{1}{\Delta z} - \frac{1}{2}\frac{\rho_1^2+\rho_2^2}{\Delta z} + \frac{3}{8}\frac{\rho_1^4+4\rho_1^2\rho_2^2+\rho_2^4}{\Delta z^5} - \frac{5}{16}\frac{\rho_1^6+9\left(\rho_1^4\rho_2^2+\rho_1^2\rho_2^4\right)+\rho_2^6}{\Delta z^7}\right.$$
$$\left. + \frac{35}{128}\frac{\rho_1^8+16\left(\rho_1^6\rho_2^2+\rho_1^2\rho_2^6\right)+36\rho_1^4\rho_2^4+\rho_2^8}{\Delta z^9} + \mathcal{O}\left(\frac{1}{\Delta z^{11}}\right)\right] \tag{53}$$

$$g(0,\rho_1,\rho_2,z_1-z_2) = f(0,\rho_1,\rho_2,z_1-z_2) \tag{54}$$

$$g(\pm1,\rho_1,\rho_2,z_1-z_2) = (2\pi)^2\left[\frac{1}{2}\frac{\rho_1\rho_2}{\Delta z^3} - \frac{3}{4}\frac{\rho_1\rho_2^3+\rho_1^3\rho_2}{\Delta z^5} + \frac{15}{16}\frac{\rho_1\rho_2^5+3\rho_1^3\rho_2^3+\rho_1^5\rho_2}{\Delta z^7}\right.$$
$$\left. - \frac{35}{32}\frac{\rho_1\rho_2^7+6\left(\rho_1^5\rho_2^3+\rho_1^3\rho_2^5\right)+\rho_1^7\rho_2}{\Delta z^9} + \mathcal{O}\left(\frac{1}{\Delta z^{11}}\right)\right] \tag{55}$$

$$g(\pm2,\rho_1,\rho_2,z_1-z_2) = (2\pi)^2\left[\frac{3}{8}\frac{\rho_1^2\rho_2^2}{\Delta z^5} - \frac{15}{16}\frac{\rho_1^2\rho_2^4+\rho_1^4\rho_2^2}{\Delta z^7} + \frac{105}{64}\frac{\rho_1^6\rho_2^2\frac{8}{3}\rho_1^4\rho_2^4+\rho_1^2\rho_2^6}{\Delta z^9}\right.$$
$$\left. - \frac{315}{128}\frac{\rho_1^2\rho_2^8+5\left(\rho_1^4\rho_2^6+\rho_1^6\rho_2^4\right)+\rho_1^8\rho_2^2}{\Delta z^{11}} + \mathcal{O}\left(\frac{1}{\Delta z^{13}}\right)\right] \tag{56}$$

$$g(\pm3,\rho_1,\rho_2,z_1-z_2) = (2\pi)^2\left[\frac{5}{16}\frac{\rho_1^3\rho_2^3}{\Delta z^7} - \frac{35}{32}\frac{\rho_1^5\rho_2^3+\rho_1^3\rho_2^5}{\Delta z^9} + \mathcal{O}\left(\frac{1}{\Delta z^{11}}\right)\right] \tag{57}$$

$$g(\pm4,\rho_1,\rho_2,z_1-z_2) = (2\pi)^2\left[\frac{35}{128}\frac{\rho_1^4\rho_2^4}{\Delta z^9} + \mathcal{O}\left(\frac{1}{\Delta z^{11}}\right)\right] \tag{58}$$

and in general

$$g(\pm\Delta m,\rho_1,\rho_2,z_1-z_2) \propto \frac{(\rho_1\rho_2)^{\Delta m}}{\Delta z^{2\Delta m+1}} \tag{59}$$

to leading order in $1/\Delta z$.

In the limit of large Δz, the integrals over the radial wavefunctions may evaluated using these expansions. This calculation is speeded by the observation that

$$\int 2\pi\rho d\rho R_{0m_1}(\rho)R_{0m_2}(\rho)\rho^n = \sqrt{\frac{2^n}{|m_1|!|m_2|!}}\Gamma\left(\frac{|m_1|+|m_2|+n}{2}+1\right) \tag{60}$$

which may be proven by using the normalization condition of the functions $R_{0m}(\rho)$ and analytically continuing the factorial function with the Gamma function. For $\Delta z < 10$ we have numerically integrated the functions f and g over the various pairs of Landau states.

After the integration over the radial and angular coordinates, the energy may now be written as expectation values of operators acting on the $Z(z)$ wavefunction. Since each electron is assumed to be in a particular Landau m level, we can calculate an effective potential energy between the electron and the nucleus by integrating over ρ, ϕ. The potential is given by Eq. 13.

The calculational strategy is similar to the single electron case. The quantum numbers ν, m for each electron are chosen ahead of time, and the wavefunction $Z(z)$ is expanded as Eq. 29 with each electron having is own variable value of a_Z. For each electron i, the matrix

$$(M_i)_{kl} = \langle \mathcal{G}_k | F(i) | \mathcal{G}_l \rangle \tag{61}$$

is calculated.

The added complication is that the diagonalization of the matrices M_i must proceed iteratively. For the given values of a_Z, the matrices are first calculated assuming that the other electrons ($j \neq i$) have $A_k = 1$ for $k = \nu_j$. Then each electron's matrix is diagonalized and the ν_ith eigenvector is used to calculate the interelectron potential for the next iteration. The matrices converge after $\sim 5-10$ iterations. Next, the values of a_Z for each electron are varied to minimize the total energy of the configuration.

For brevity, we discuss the ground state energies and wavefunctions for H_2, He and HHe as a function of field strength for $\beta \geq 1000$. For the molecules we again take the molecular axis to be aligned with the magnetic field direction. Since we are interested in the ground states of these species we set $\nu = 0$ for all the electrons and assign the electrons consecutive m quantum numbers beginning with $m = 0$. Because none of the electrons have axial excitations, we are interested in only the most negative eigenvalue of the electron matrices. This eigenvalue is more efficiently determined by varying the coefficients in Eq. 29 directly than by diagonalizing the electron matrices iteratively.

Table IV gives the binding energies of the most tightly bound states of H_2, He, HHe and H calculated numerically using the variational method. The energies for H are within 1.1 % of the values quoted by Ruder *et al.* [3] for weakest field strength common between the two studies. For the stronger fields, the agreement is even closer. For He the energies are within 2.5 % of the values of Ruder *et al.* for the fields that overlap.

We also computed the binding energies of H_2 and H^- and compared the results with the values found by Lai *et al.* [6]. We interpolated the Lai *et al.* results using a cubic spline with $\ln\beta$ as the independent variable. The binding energies for H_2 were within $0.6-3\%$ of the Lai *et al.* results. The agreement for H^- was poorer ranging from $2-7\%$. The results for H and H_2^+ (Table II) agree to within 0.9% of the Lai *et al.* values.

We compare these interpolated results with the results for the species He, HHe and HHe^+ to find that the reaction

$$H + He \rightarrow HHe \tag{62}$$

is exothermic over the range of field strengths considered. However, if there is sufficient hydrogen present, the species HHe would quickly be consumed by the exothermic reaction

$$H + HHe \rightarrow He + H_2 \tag{63}$$

for these field strengths, unless

$$H + HHe \rightarrow H_2He \tag{64}$$

is sufficiently exothermic (the binding energy and configuration of H_2He is beyond the scope of this paper). The potential production channels for HHe^+,

$$He + H_2 \rightarrow HHe^+ + H^-, \tag{65}$$

$$He + H_2^+ \rightarrow HHe^+ + H \text{ and} \tag{66}$$

$$He + H \rightarrow HHe^+ + e^- \tag{67}$$

are endothermic over the range of field strengths considered. We therefore conclude that at least for hydrogen and helium, atoms in an intense magnetic field are far more cohesive than adhesive.

B. Validity of the Born-Oppenheimer Approximation

When studying molecules in a intense magnetic field, we have assumed that the nuclear motion and the electronic motion decouple, *i.e.* the Born-Oppenheimer approximation. Schmelcher *et al.* [12] have examined the validity of this approximation in the presence of a strong magnetic field. They performed a pseudoseparation of the equations of motion and derive electronic and nuclear equations of motion. Because we have assumed throughout that the nuclei are infinitely massive and that the molecules are aligned with the magnetic field, the corrections to the Born-Oppenheimer approximation may be neglected. However, the techniques outlined here, specifically the use of one-dimensional Coulomb wavefunctions and Gauss-Hermite functions as a convenient and compact basis for the electronic wavefunctions of atoms and molecules in intense magnetic fields, can be extended to the more general case where these restrictions have been relaxed.

VI. CONCLUSIONS

We have developed both an analytic and a convenient numerical technique to accurately calculate the properties of simple atoms and molecules in an intense magnetic field. The calculations presented here complement the earlier work. We examine two compounds (HHe and HHe^+) in addition to the species studied earlier which may form in the intensely magnetized outer layers of a neutron star. Additionally, our technique finds both tightly bound and excited states efficiently and accurately which is necessary to calculate the radiative transfer of the neutron star atmosphere.

The techniques presented in this paper complement the recent work in this area. They provide moderately high precision with little computational or algebraic expense. Most recent work has focussed on extremely high precision by using a Hartree-Fock-like method to reduce the three-dimensional problem to three coupled one-dimensional problems. Generally, two of the one-dimensional equations are solved over an functional basis, *i.e.* Legendre polynomials [13] or spherical harmonics [14], and the radial differential equation is solved numerically over a pointlike basis. Fassbinder *et al.* [15] and Shertzer *et al.* [16,17] use a finite element method throughout.

The spirit of the work presented here is different. We have solved for the wavefunctions using a basis for all three coordinates: the Landau wavefunctions in the angular and radial direction and the one-dimensional Coulomb wavefunctions or the Gauss-Hermite functions along the axis of the magnetic field. The power of this technique is that the basis functions resemble the actual wavefunctions and preserve the symmetries of the potential; consequently only a few basis functions ($\sim 1-2$ and ~ 20 respectively) are require to reach moderately high precision.

The work of Kravchenko *et al.* [18,19] takes an orthogonal approach and achieves very high precision by solving the general problem of a hydrogen atom in an arbitrarily strong magnetic field with a double power series in $\sin\theta$ and r. It remains to be seen whether this simple and accurate technique can be applied to more general problems.

The properties of the lowest density layers of a neutron star's crust determine the spectral characteristics of the radiation expected from the star. One possibility is that linear chains of atoms form in the surface layers [20–24,6], and the atmosphere condenses at finite density. We find that the reactions between hydrogen and helium are unlikely to affect the formation of hydrogen or helium chains unless the formation of hydrogen-helium hybrid chains is favored.

If the envelope is truncated at sufficiently high density, the thermal isolation of the core can be substantially reduced [25]. Furthermore, the composition of the outermost layers determines the spectra from the neutron star (*e.g.* [26–29]). Without understanding magnetized chemistry in neutron-star atmospheres, is difficult to interpret observations of these objects.

---

[1] R. Loudon, Am. J. Phys. **27**, 649 (1959).
[2] L. K. Haines and D. H. Roberts, Am. Journ. Phys. **37**, 1145 (1969).
[3] H. Ruder *et al.*, *Atoms in Strong Magnetic Fields : Quantum Mechanical Treatment and Applications in Astrophysics and Quantum Chaos* (Springer-Verlag, New York, 1994).
[4] L. D. Landau and E. M. Lifshitz, *Quantum Mechanics : Non-Relativistic Theory*, 3rd ed. (Pergamon, Oxford, 1989).
[5] V. Canuto and D. C. Kelly, Astr. Sp. Sci. **17**, 277 (1972).
[6] D. Lai, E. E. Salpeter, and S. L. Shapiro, Phys. Rev. A. **45**, 4832 (1992).
[7] M. Abramowitz and I. A. Stegun, *Handbook of Mathematical Functions* (Dover, New York, 1970).
[8] B. H. Bransden and C. J. Joachain, *Introduction to Quantum Mechanics* (Longman, Harlow, England, 1989).
[9] J. C. Le Guillou and J. Zinn-Justin, Ann. Phys. **154**, 440 (1984).

[10] J. C. Lopez, P. Hess, and A. Turbiner, astro-ph/9707050 (unpublished).
[11] W. H. Press, B. P. Flannery, S. A. Teukolsky, and W. T. Vettering, *Numerical Recipes in C*, 1st ed. (Cambridge Univ. Press, Cambridge, 1988).
[12] P. Schmelcher, L. S. Cederbaum, and H.-D. Meyer, Phys. Rev. A **38**, 6066 (1988).
[13] V. Melezhik, Phys. Rev. A **48**, 4528 (1993).
[14] M. D. Jones, G. Ortiz, and D. M. Ceperly, Phys. Rev. A **54**, 219 (1996).
[15] P. Fassbinder *et al.*, Phys. Rev. A **53**, 2135 (1996).
[16] J. Shertzer *et al.*, Phys. Rev. A **39**, 3833 (1989).
[17] J. Shertzer *et al.*, Phys. Rev. A **40**, 4777 (1990).
[18] Y. Kravchenko *et al.*, Phys. Rev. A **54**, 287 (1996).
[19] Y. Kravchenko *et al.*, Phys. Rev. Lett. **77**, 619 (1996).
[20] M. A. Ruderman, in *Physics of Dense Matter*, edited by C. J. Hansen (Reidel, Dordrecht, Holland, 1974).
[21] H.-H. Chen, M. A. Ruderman, and P. G. Sutherland, ApJ **191**, 473 (1974).
[22] E. G. Flowers *et al.*, ApJ **215**, 291 (1977).
[23] E. Müller, A&A **130**, 415 (1984).
[24] D. Neuhauser, S. E. Koonin, and K. Langanke, Phys. Rev. A **36**, 4163 (1987).
[25] L. Hernquist, MNRAS **213**, 313 (1985).
[26] G. G. Pavlov, Y. A. Shibanov, J. Ventura, and V. E. Zavlin, A&A **289**, 837 (1994).
[27] G. G. Pavlov, V. E. Zavlin, J. Trümper, and R. Neuhäuser, astro-ph/9609097 (unpublished).
[28] V. E. Zavlin, G. G. Pavlov, and Y. A. Shibanov, A& A **315**, 141 (1996).
[29] M. Rajagopal, R. W. Romani, and M. C. Miller, ApJ **479**, 347 (1997).

TABLE I. The zeroth and first-order binding energies of hydrogen in an intense magnetic field in Rydberg units

	$\|000\rangle$		$\|0-10\rangle$		$\|0-20\rangle$		$\|001\rangle$		$\|002\rangle$	
β	E_0	E_1	E_0	E_1	E_0	E_1	E_0	E_1	E_0	E_1
1×10^3	15.58	18.48	10.45	13.71	8.779	11.76	0.9401	0.9888	0.5841	0.6215
2×10^3	18.80	22.26	12.81	16.73	10.83	14.46	0.9559	0.9935	0.6062	0.6322
5×10^3	23.81	28.09	16.57	21.51	14.12	18.73	0.9710	0.9970	0.6329	0.6560
1×10^4	28.22	33.19	19.94	25.73	17.10	22.55	0.9790	0.9983	0.6518	0.6730
2×10^4	33.21	38.91	23.81	30.53	20.56	26.93	0.9849	0.9990	0.6684	0.6880
5×10^4	40.75	47.49	29.76	37.81	25.91	33.61	0.9903	0.9996	0.6885	0.7060
1×10^5	47.20	54.76	34.95	44.08	30.60	39.40	0.9931	0.9998	0.7027	0.7188

TABLE II. The binding energy of H_2^+ in an intense magnetic field. The values have been derived numerically and the final column gives the numerically derived binding energy of the ground state of H for comparison.

	H_2^+		H
β	$\|000\rangle$	$\|0-10\rangle$	$\|000\rangle$
1×10^3	28.35	20.43	18.57
2×10^3	35.04	25.63	22.37
5×10^3	45.77	34.08	28.25
1×10^4	55.37	41.83	33.37
2×10^4	66.56	50.86	39.11
5×10^4	83.45	64.95	47.70
1×10^5	98.27	77.38	54.96

TABLE III. The binding energy of H_2^+ in an intense magnetic field for comparison with the results of Lopez *et al.* [10].

	H_2^+		H
B (G)	$\|000\rangle$	$\|0-10\rangle$	$\|000\rangle$
1×10^{11}	7.347	4.880	5.611
5×10^{11}	13.37	9.188	9.568
1×10^{12}	17.05	11.88	11.87
2×10^{12}	21.53	15.25	14.58
5×10^{12}	28.89	20.85	18.89
1×10^{13}	35.69	26.14	22.74

TABLE IV. The binding energy of He, HHe^+ and HHe in an intense magnetic field. The number in parenthesis gives the number of free parameters in each variational model. The electrons occupy the most tightly bound states, $|0m0\rangle$, *e.g.* $|000\rangle$, $|0-10\rangle$ and $|0-20\rangle$ for HHe. The values have been derived numerically and the final column gives the numerically derived binding energy of the ground state of H for comparison.

β	He (6)	HHe^+ (5)	HHe (7)	H (25)
1×10^2	32.47	35.75	42.59	9.383
2×10^2	40.98	45.95	54.25	11.64
5×10^2	54.95	63.07	73.36	15.28
1×10^3	67.85	79.24	90.89	18.57
2×10^3	83.00	98.55	111.3	22.37
5×10^3	106.9	129.7	143.1	28.25
1×10^4	127.8	157.5	168.0	33.37
2×10^4	151.6	189.7	193.1	39.11
5×10^4	187.6	239.6		47.70
1×10^5	218.4	282.5		54.96

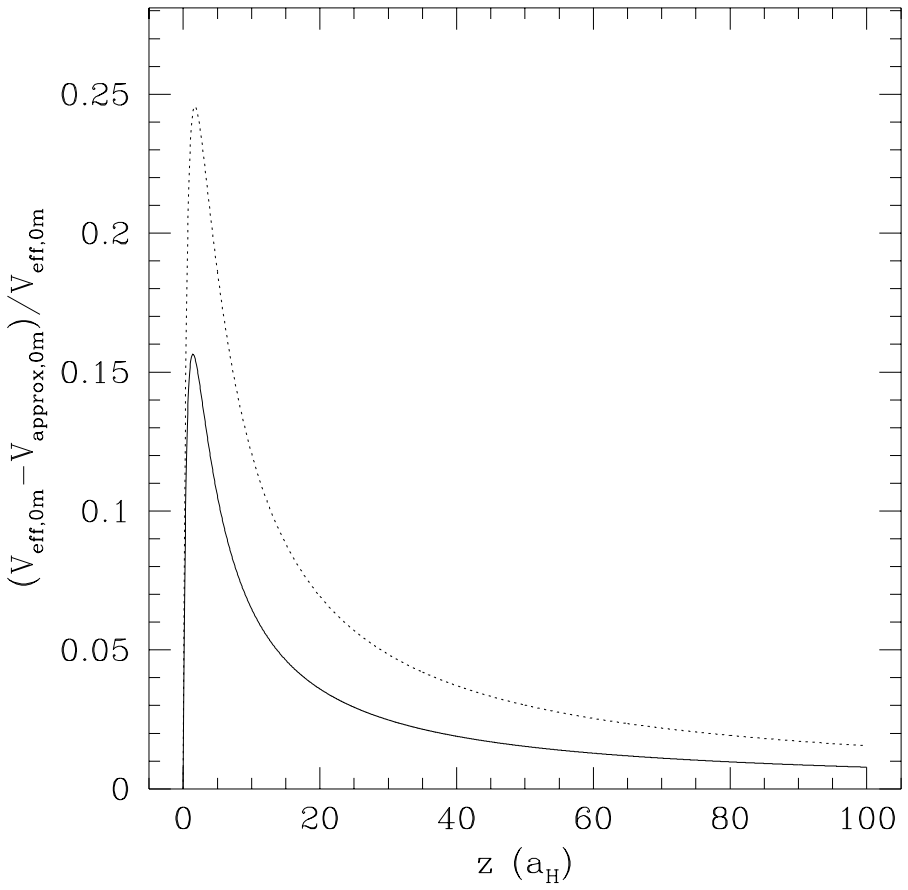

FIG. 1. The relative difference between the effective potential and the approximated potential. The solid line traces the difference for the $m = 0$ state and the dotted line gives the $m = -1$ state.

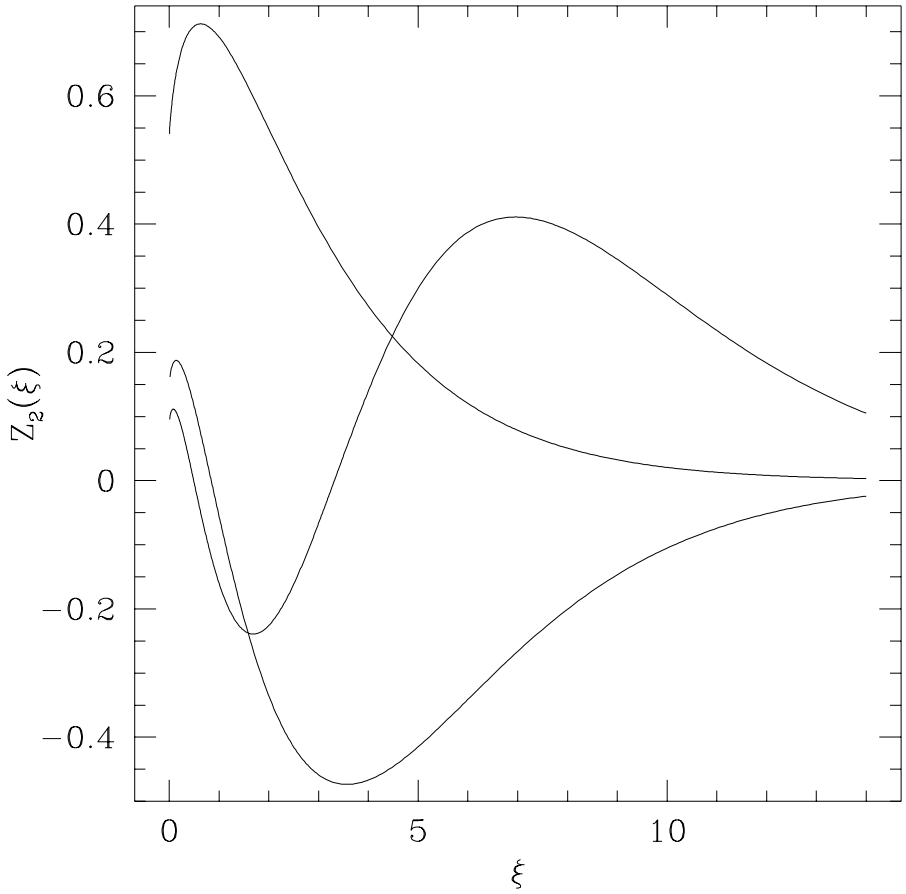

FIG. 2. The function $Z_2(\xi)$ for $\xi_0 = 0$ for $nZ = 1/2, 3/2, 5/2$.

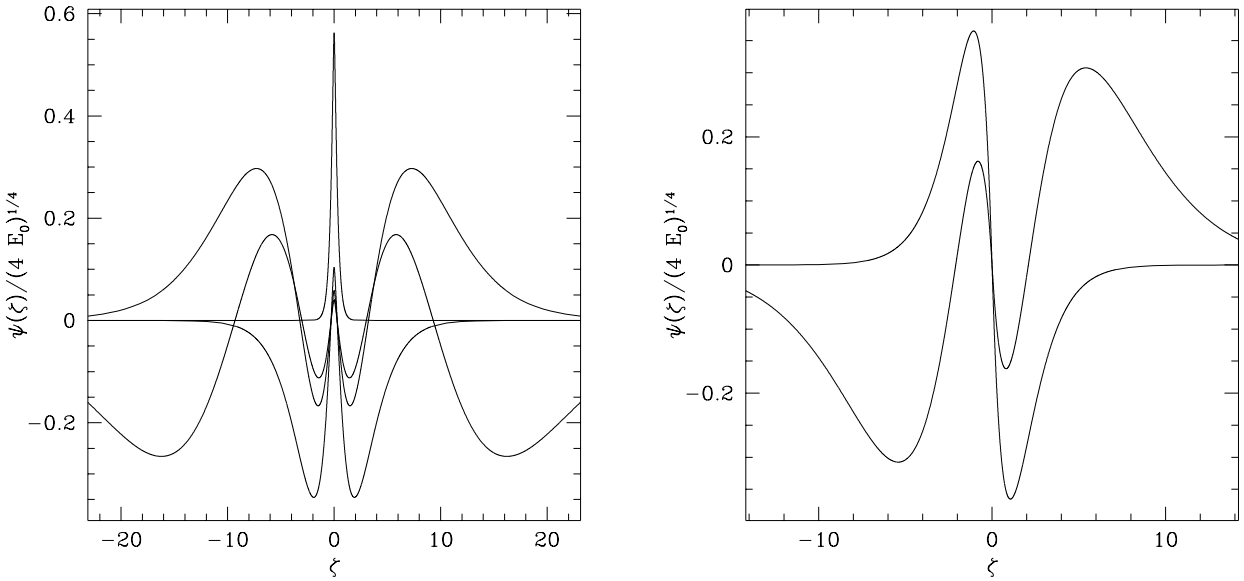

FIG. 3. The axial wavefunctions of hydrogen in an intense magnetic field (analytic calculation) for $\beta = 1000$. The left panel depicts the first four even states with axial excitations ($|000\rangle, |002\rangle, |004\rangle, |006\rangle$). The right panel shows the first two odd states ($|001\rangle, |003\rangle$).

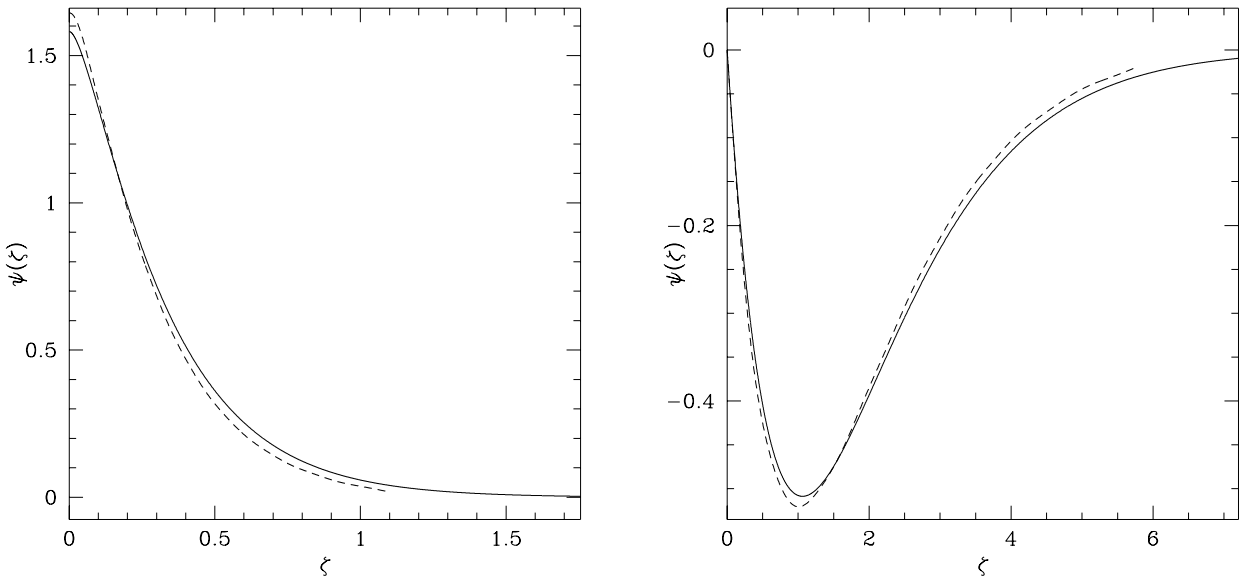

FIG. 4. A comparison of numerical and analytic wavefunctions for hydrogen. Both panels are for $\beta = 1000$. The left panel displays the state $|000\rangle$, and the right shows $|001\rangle$. The dashed line traces the numerical results with the first 31 $\mathcal{G}_k$. The solid line traces the zeroth-order analytic solutions.

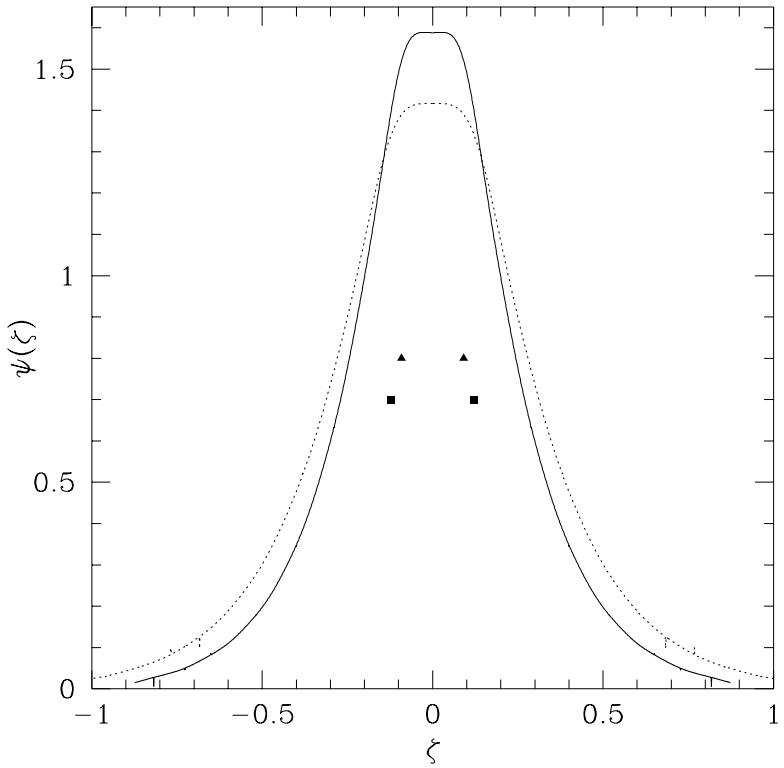

FIG. 5. The ground and first-excited state of H_2^+. The solid line traces $|000\rangle$, and the dashed line follows $|0-10\rangle$. The triangles give the positions of the protons for the ground state and the squares for the excited state.